

Article

Tuning the Electronic and Charge Transport Properties of Schiff Base Compounds by Electron Donor and/or Acceptor Groups

Ahmad Irfan ^{1,2,*}, Abdullah G. Al-Sehemi ¹  and Abul Kalam ¹

¹ Department of Chemistry, College of Science, King Khalid University, P.O. Box 9004, Abha 61413, Saudi Arabia

² Research Center for Advanced Materials Science, College of Science, King Khalid University, P.O. Box 9004, Abha 61413, Saudi Arabia

* Correspondence: irfaahmad@gmail.com; Tel.: +966-172419481

Abstract: Organic semiconductors have gained substantial interest as active materials in electronic devices due to their advantages over conventional semiconductors. We first designed four Schiff base compounds, then the effect of electron donor/acceptor groups (methyl/nitro) was studied on the compounds' electronic and transport nature. The absorption spectra (λ_{abs}) were computed by time-dependent DFT at TD-B3LYP/6-31+G** level. The effect of different solvents (ethanol, DMF, DMSO, and acetone) was investigated on the λ_{abs} . The substitution of the -NO₂ group to the furan moiety at the 5th position in Compound 3 leads to a red-shift in the absorption spectrum. A smaller hole reorganization energy value in Compound 3 would be beneficial to get the hole's intrinsic mobility. In contrast, a reduced-electron reorganization energy value of Compound 4 than hole may result in enhanced electron charge transfer capabilities. The reorganization energies of compounds 1 and 2 exposed balanced hole/electron transport probability. The optical, electronic, and charge transport properties at the molecular level indicate that Compound 3 is suitable for organic electronic device applications.



Citation: Irfan, A.; Al-Sehemi, A.G.; Kalam, A. Tuning the Electronic and Charge Transport Properties of Schiff Base Compounds by Electron Donor and/or Acceptor Groups. *Materials* **2022**, *15*, 8590. <https://doi.org/10.3390/ma15238590>

Academic Editors: Martin Weis and Jung-Kul Lee

Received: 20 September 2022

Accepted: 20 November 2022

Published: 2 December 2022

Publisher's Note: MDPI stays neutral with regard to jurisdictional claims in published maps and institutional affiliations.



Copyright: © 2022 by the authors. Licensee MDPI, Basel, Switzerland. This article is an open access article distributed under the terms and conditions of the Creative Commons Attribution (CC BY) license (<https://creativecommons.org/licenses/by/4.0/>).

Keywords: organic field-effect transistors; schiff base compounds; density functional theory; optoelectronic properties; charge transport

1. Introduction

Organic semiconductor materials (OSMs) have become very important due to their flexible, cheap, lightweight, and environmentally friendly nature [1–3]. Small OSMs are attracting interest because of their ease of synthesis, light weight, and inexpensive cost. The ability to interact with solvents and associated molecules for various modes of charge transport makes them beneficial for promising optoelectronic applications [4].

Developments in OSMs in organic field-effect transistors (OFETs), organic light-emitting diodes (OLEDs), photodiodes, and photovoltaics have persuaded the researchers to develop them into functional materials [5–7]. The OFETs with better performance may be achieved by the development of device fabrication approaches as well as by new materials [8]. Tuning excellent charge-transport properties in molecular systems is feasible by enhancing intermolecular interactions, resulting in rearranged optical and electronic structures. Thus, developing intermolecular interactions can be an efficient approach to enhance OFETs performance. To improve the intermolecular interactions of OSMs, heteroatoms like O, S, N and C=C or C≡C were substituted in the π -conjugated backbone. The existence of π -conjugation leads to the delocalization of electrons adjacent to the core and the prospect of superior charge carrier mobility [9–12]. OSMs are amalgamated by weak intermolecular interactions, like van der Waals, π - π , S–S, and C–H [13].

The OSM versatility delivers numerous exciting characteristics to be tuned. Since organic materials such as Schiff derivatives have potential in semiconductors, they have attracted great interest. Conjugated Schiff bases have thrilling properties and were used in

numerous electronics [14,15], OFETs [16], and electrochromic devices [17]. The significant progress of electronic materials and devices in recent years has shown that the use of Schiff bases as electronic materials offers significant excellent advantages, and their facile synthetic process made them a potential alternative for electronic devices. The superior thermal strength, broader absorption, smaller band gap, and great electrical conductivity also ensures that Schiff bases will be used as future materials for organic electronics. The Schiff base compounds demonstrate intramolecular proton transfer and donor-acceptor combination.

Moreover, donor- π -bridge-acceptor and heteroatoms in these compounds govern the electronic transitions to make them appealing for semiconductors [17–20]. The specific feature of Schiff bases is their solvatochromic behavior. The π -conjugation leads to delocalization in these compounds resulting in superior mobility in OFETs. Moreover, donor and acceptor groups as substituents augment the electronic, solvatochromic, and optical properties [21].

The effect of the electron-donating group (methyl), the electron-withdrawing group (nitro), and solvents with various polarities (ethanol, DMF, DMSO, and acetone) were examined on the absorption spectra for designed Schiff base compounds, see Figure 1. The donor and acceptor effect on the electronic and charge transport properties, e.g., frontier molecular orbitals, molecular electrostatic potential (MEP), and reorganization energy, is ascertained by DFT and time dependent DFT.

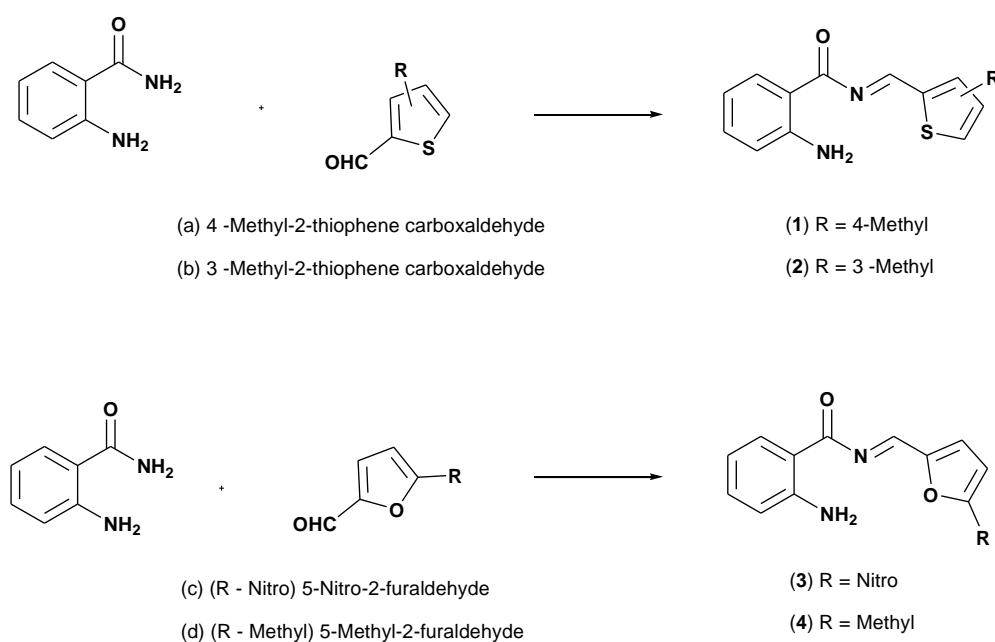


Figure 1. The structures of Schiff base compounds.

2. Computational Details

Quantum chemical approaches have proven efficient at exploring the structure–properties relationship. Computational investigations have played a substantial role in probing the properties of OSMs [22]. Computational methods are used to analyze materials' properties in different fields [23]. It has been shown in previous studies that the density functional theory (DFT) is a rational choice for investigating the charge transport and optoelectronic properties of OSMS [24]. Moreover, quantum chemical calculations were utilized to ascertain the properties of thiophene-base compounds [25,26]. Optimization of Schiff base compounds in the ground state (S_0) was accomplished by DFT [27–30] at the B3LYP/6-31+G** level, as the B3LYP functional demonstrated good results compared with reported data [31,32]. The electron affinity, ionization potential, [33] and reorganization energy (hole/electron) values were estimated at the B3LYP/6-31+G** level. Time-dependent DFT [34] was applied to calculate the absorption (λ_{abs}) by TDDFT [35] the TD-B3LYP/6-

31+G** level in gas and solvents (acetone, ethanol, DMSO, and DMF) using the Gaussian16 package [36].

3. Results and Discussion

3.1. Electronic Properties

The LUMO (E_{LUMO}) and HOMO (E_{HOMO}) and their energy gaps (E_{gap}) are essential parameters to understand the optoelectronic and charge transport of compounds. Here, we have tabulated the E_{HOMO} , E_{LUMO} , and E_{gap} of Schiff base compounds at S_0 in Table 1. The electron-withdrawing group nitro instead of methyl was critical for adjusting the frontier molecular orbital (FMO) energy value in Comp3. Substitution of the nitro group reduces the E_{HOMO} and E_{LUMO} values of Comp3 and decreases E_{gap} , i.e., 2.07 eV.

Table 1. The LUMO energies (E_{LUMO}), HOMO energies (E_{HOMO}), and energy gaps (E_{gap}) (in eV) of Schiff base compounds at B3LYP/6-31+G** level.

Comp.	E_{HOMO}	E_{LUMO}	E_g
1	−5.65	−2.68	2.97
2	−5.62	−2.64	2.98
3	−5.88	−3.81	2.07
4	−5.55	−2.55	3.00

The charge densities distribution of FMOs are illustrated in Figure 2. The HOMO is delocalized on aminobenzene while LUMO is localized on thiophene/furan moiety in 1/2 and 3/4. Moreover, LUMO can also be found at nitro group in 3 which is revealing an intra-molecular charge transfer (ICT) from H → L.

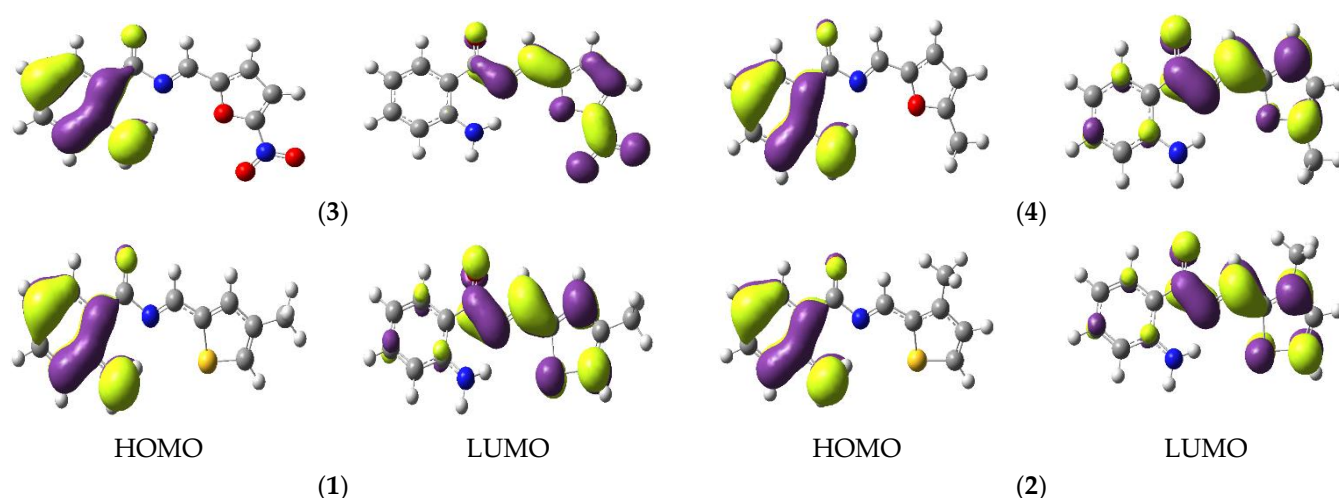


Figure 2. The ground state contours of FMOs (HOMOs and LUMOs) of Schiff derivatives (contour value = 0.035).

The work functions (ϕ) of Ag (Al) are 4.74 (4.08 eV) [37]. The electron/hole injection energies (EIE/HIE) barrier was disclosed from Schiff base compounds to the Al/Ag electrode individually, which were assessed as $(E_{LUMO}-\phi)$ and $(\phi-E_{HOMO})$, respectively. The estimated EIE barrier from Compounds 1–4 to Al are 1.40, 1.44, 0.27, and 1.53 eV, while HIE for 1–4 is 1.57, 1.54, 1.80, and 1.47 eV, respectively. The calculated EIE from 1–4 to Ag are 2.06, 2.02, 0.93, and 2.19 eV, respectively. The HIE for 1–4 are 0.91, 0.88, 1.14, and 0.81 eV. These findings uncovered that substituting the nitro group at the 5th position on the furan group in 3 would be promising to improve the electron injection. In contrast, the methyl group could complement the hole injection ability, see Table 2.

Table 2. The hole/electron injection energy (EIE/HIE) barriers from of Schiff base compounds to Silver (Ag)/Aluminum (Al) electrodes were assessed at B3LYP/6-31+G** level.

Comp.	HIE (Ag)	EIE (Ag)	HIE (Al)	EIE (Al)
1	0.91	2.06	1.57	1.40
2	0.88	2.02	1.54	1.44
3	1.14	0.93	1.80	0.27
4	0.81	2.19	1.47	1.53

3.2. Absorption Spectra

Absorption (λ_{abs}) and the percent contribution of the transitions and oscillator strengths (f) involved by FMOs of Schiff base derivatives at TD-B3LYP/6-31+G** level in the gas phase and several solvents are tabulated in Table 3. The solvent effect has attracted much attention because many chemical processes occur in the solution phase. To study the impact of the solvent on absorption maxima, the gas phase studies have been made of molecules (as a control), and then the data were compared with the λ_{abs} and computed in a solvent such as ethanol, acetone, DMF, and DMSO.

Table 3. The absorption wavelengths (λ_{abs} , nm), oscillator strengths (f), %Contribution (%Con), and main transitions in the gas phase as well as in solvents (ethanol, acetone, DMF, and DMSO) of Schiff base compounds at TD-B3LYP/6-31+G** level.

Comp.	λ_{abs}	f	Tran	%Con	λ_{abs}	f	Tran	%Con
Gas Phase								
1	512	0.0432	H → L	71%	477	0.0721	H → L	71%
	316	0.2682	H → L+1	34%	334	0.4736	H → L+1	12%
2	510	0.0439	H → L	71%	474	0.0740	H → L	70%
	312	0.2970	H → L+1	47%	325	0.6117	H → L+1	60%
3	745	0.0259	H → L	71%	680	0.0343	H → L	70%
	410	0.0518	H → L+1	16%	334	0.5260	H → L+2	10%
4	502	0.0507	H → L	70%	468	0.0860	H → L	70%
	308	0.4157	H → L+1	37%	330	0.7663	H → L+1	12%
	230	0.0632	H → L+2	28%	240	0.0918	H → L+1	2%
In Acetone								
1	478	0.0717	H → L	70%	477	0.0747	H → L	70%
	334	0.4744	H → L+1	12%	335	0.4839	H → L+1	12%
2	474	0.0736	H → L	70%	474	0.0769	H → L	70%
	325	0.6109	H → L+1	60%	326	0.6271	H → L+1	60%
3	682	0.0342	H → L	71%	682	0.0342	H → L	71%
	334	0.4860	H → L+2	9%	335	0.5838	H → L+2	9%
4	468	0.0855	H → L	70%	468	0.0893	H → L	70%
	330	0.7661	H → L+1	13%	332	0.7773	H → L+1	12%
	240	0.0918	H → L+1	2%	240	0.0921	H → L+2	3%
In DMSO								
1	477	0.0745	H → L	70%				
	335	0.4808	H → L+1	12%				
2	473	0.0766	H → L	70%				
	326	0.6244	H → L+1	60%				
3	678	0.0352	H → L	71%				
	335	0.5819	H → L+2	9%				
4	467	0.0891	H → L	70%				
	331	0.7750	H → L+1	12%				
	240	0.0926	H → L+2	3%				

Here, we noticed that the first and second λ_{abs} peaks at 512 nm and 316 nm corresponded to $H \rightarrow L$ ($S_0 \rightarrow S_1$) and $H \rightarrow L+1$ for **1** in the gas phase, whereas the first and second λ_{abs} peaks were observed at 477 nm, corresponding to $H \rightarrow L$ ($S_0 \rightarrow S_1$) and 334 nm from $H \rightarrow L+1$ for **1** in ethanol. The effect of ethanol solvent in **1** was observed on λ_{abs} from the gas phase to ethanol, i.e., the first peak is 35 nm blue shifted while the second peak is 18 nm red shifted, respectively. The solvent polarity has no significant effect on λ_{abs} (see Table 3). In the gas phase, the substitution of the nitro group at the 5th-position of furan in **3** leads to a red shift, i.e., 233 nm in the first band and 94 nm in the second band as compared to **1**. The significant effect on the first peak was observed in λ_{abs} from the gas phase to ethanol in **3** which is being blue-shifted, i.e., 65 nm. The substitution of the nitro group at 5th-position of furan in **3** leads to a blue shift in λ_{abs} from the gas phase to acetone, DMF, and DMSO, i.e., 63, 63, and 67 nm for the first band, respectively. The effect of electron acceptor and electron donor moiety is mainly on the first λ_{abs} band, i.e., the substitution of the electron deactivating group (nitro) at the 5th-position of furan in **3** tune the λ_{abs} wavelength toward a shorter wavelength.

All electronic transitions and corresponding oscillator strengths in the absorption spectra are π to π^* type. A fascinating tendency in the oscillator strength was noticed for Schiff base compounds: the oscillator strengths for $S_0 \rightarrow S_1$ are prodigiously larger in the solvent phase as compared to the gas phase. Furthermore, λ_{abs} indicates that **3** has a band in the visible region. According to the nature of the transition, the HOMO to LUMO transition was observed for the first excitation. The λ_{abs} wavelengths are listed in Table 3. All the compounds exhibit two absorption peaks related to the aminobenzene and the charge transfer associated with the thiophene/furan substituted moiety (Figure 2). The first bands may be attributed to a charge transfer-type transition (CT) of the π to π^* , and from the HOMO located on aminobenzene to the LUMO on the thiophene-furan part. The lowest energy gaps are the π to π^* for the **3** (2.07 eV), while the other Schiff based derivatives showed larger band gaps as established from the optical property values and the occurrence of UV values (see Table 3). These results clearly show that the interaction between the donor and the acceptor, either in an alternating manner or in a separate block in the molecule, performs a significant role in controlling the planarity and the photophysical properties.

3.3. Charge Transport Properties

Charge transports are sensitive to internal traps, as well as transport within *p*-type materials from low ionization potential levels, making the filling of deep traps less attractive. Likewise, materials of *n*-type benefit from a larger EA, where there are also few available traps. The hole injection from an electrode to a semiconductor HOMO is more effective when the electrode is closer, or even greater than a semiconductor IP. Similarly, for better electron injection, the larger EA values would be suitable. For the better stability of the device, it is certified that its charged and neutral states do not contribute to chemical reactions [38]. To preclude a thermodynamically efficient reaction (which contains oxygen and water), a neutral semiconductor is expected to require IP greater than 4.9 eV [38]. The shallow HOMO may diminish ambient O_2 in the H_2O existence to form OH^- . The semiconductors having deep HOMO can receive holes that can oxidize the H_2O in the atmosphere. Obstacles during such an undesirable reaction by chance lead to overpotentials that permit organic semiconductors to make redox gently so that they can unveil the stabilities. Electron transport is most affected by the reaction with air, and it is important to prevent the electron polaron from degrading the material. To achieve this, the LUMO has to be low to avert excited electrons to reduce the water-soluble O_2 systems to O_2^- [39] or H_2O to OH^- . These undesirable electrochemical processes can reduce charge transfer and set about irreversible changes within the semiconductor. Defining the exact amount of EA that needs to be skipped to prevent this redox reaction requires consideration of the maximum response power and device morphology. It has been suggested that high EA can put down oxidation reactions [40].

The values of the ionization potential (IPs) and the electron affinity (EAs) are among the most important factors of organic compounds for use in OFETs, xerography, and electroluminescence. These parameters have been interconnected to the amount of energy required to add or remove electrons and thus can be considered as molecular stability with respect to donating or receiving electrons to create an exciton. We describe the assessed IPs and EA for the Schiff base derivatives, see Table 4. Additionally, it entails that there was a positive correlation between the LUMO level and EAs. The π -conjugated organic materials with an electronic charge motion are carried out by a hopping mechanism. The internal reorganization energy (λ_{int}), because of its structural variation from neutral to ionic states (cation and/or anion), is a vital parameter for the charge transfer in organic electronic materials, as it is one of the most important factors that influence the rate of the charge of hopping and considering the mobility of field-effect transistors. In order to have a high degree of mobility of materials, the λ_{int} needs to be reduced. The λ_{int} is a significant parameter for the estimation of the rate of charge transfer. Previously, it was exposed that the DFT can be a trustworthy way to imitate the experimental data [41–44]. The λ_{int} and external polarization (λ_{ext}) are two components of total reorganization energy [45]. Here, λ_{int} was projected for the hole (λ_{hole}) and the electron (λ_{elec}). The λ_{hole} was estimated by Equations (1) and (2) [46]:

$$\lambda_1 = E^+(B) - E^+(B^+) \quad (1)$$

$$\lambda_2 = E(B^+) - E(B) \quad (2)$$

where $E^+(B)$, $E^+(B^+)$, $E(B^+)$, and $E(B)$ are the energies of the cation at neutral optimized geometry, neutral at the cationic optimized geometry, optimized cation, and optimized neutral geometry, respectively. Correspondingly, λ_{elec} was estimated by Equations (3) and (4):

$$\lambda_3 = E^-(B) - E^-(B^-) \quad (3)$$

$$\lambda_4 = E(B^-) - E(B) \quad (4)$$

where $E^-(B)$, $E^-(B^-)$ and $E(B^-)$ are energies of the anion at neutral optimized geometry, neutral at anionic optimized geometry, and the anionic optimized geometry.

Table 4. Vertical/adiabatic ionization potential (IP_v/IP_a), electron affinity (EA_v/EA_a), and hole/electron reorganization energies ($\lambda_{hole}/\lambda_{elec}$) in eV of Schiff derivatives at B3LYP/6-31+G(d,p) level.

Comp.	IP_a	EA_a	IP_v	EA_v	λ_{hole}	λ_{elec}	$\Delta\lambda$
1	7.07	1.47	7.37	1.19	0.533	0.527	0.006
2	7.04	1.48	7.35	1.17	0.542	0.541	0.001
3	7.34	2.55	7.61	2.22	0.479	0.630	0.151
4	6.98	1.28	7.26	1.03	0.522	0.477	0.045

The vertical and adiabatic EA and IP were computed by using Equations (5) and (6).

$$\text{Adiabatic} \begin{cases} IP_a = E(B^+) - E(B) \\ EA_a = E(B) - E(B^-) \end{cases} \quad (5)$$

$$\text{Vertical} \begin{cases} IP_v = E^+(B) - E(B) \\ EA_v = E(B) - E^-(B) \end{cases} \quad (6)$$

The computed λ_{hole} , λ_{elec} and λ_{int} of Schiff base derivatives at the level of B3LYP/6-31+G** are shown in Table 4. The smaller the electron reorganization energy value of the compound exposed that it would be suitable as an *n*-type semiconductor, while the smaller hole reorganization energy value of the compound uncovered that it would be appropriate as a *p*-type semiconductor; details can be found in reference 43. The λ_{hole} and λ_{elec} values for 1 and 2 reveal that these compounds might be good, having balanced hole and electron

transfer mobility, and the ability to be used in *p* and *n*-type materials. The λ_{hole} has been calculated to be much smaller than the λ_{elec} with the difference in the range of 0.151 eV for **3**, which reveals that this compound might be a suitable *p*-type contender. The λ_{elec} has been calculated to be smaller than the λ_{hole} with the difference in the range of 0.045 eV for **4** which shows that this compound might be suitable as *n*-type contender. Hitherto, it was pointed out that lower λ_{int} values can increase the charge transfer rate [43,47–49]. The substitution of the electron-deactivating group (nitro) at the 5th-position of the furan in **3** leads to a decrease in the polarization of the neutral to cation state which means that there are lower λ_{hole} values compared to other compounds, suggesting that this compound could be a good choice for the hole transfer. It may turn out that the electron activating group (methyl) at the 5th-position of furan in **4**, leads to a decrease of the polarization of the neutral to anion which will result in a lower λ_{elec} value in comparison with other compounds, which suggests that this compound may be a good candidate for electron transport.

3.4. Molecular Electrostatic Potential

Earlier works reported that diffraction methods would be supportive in determining molecular electrostatic potential (MEP) experimentally, and this can also be tested by simulation. The MEP points to the widespread electronic distribution across the board, which is a broad aspect of understanding and predicting the reactivity of different compounds. In Figure 3, the MEP map can be seen in the color scheme. Red represents regions with a high negative potential and blue indicates regions with high positive potential. High potential of negative regions is ideal for electrophilic attacks, however, high potential regions of positive prefer nucleophilic attacks. The MEP decreases with order blue > green > yellow > orange > red; red indicates the most repulsion while blue indicates the most attractive phase of the nucleophilic attack and vice versa.

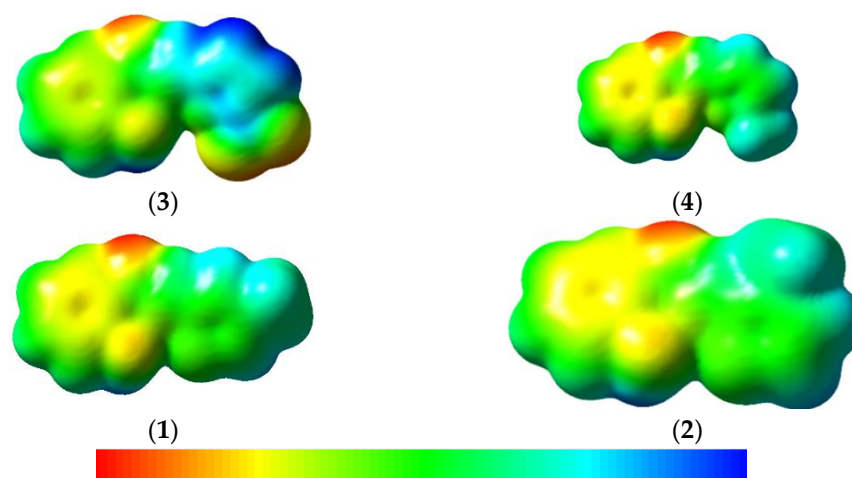


Figure 3. Molecular electrostatic potential views of Schiff base compounds.

From Figure 3, it was revealed that keto oxygen has negative potential in all the Schiff base compounds. The nitro group in **3** has also negative potential, while the $-NH_2$ group has good positive potential in all the Schiff base derivatives. In **3**, the nitro group will have a negative potential. These results clearly indicate that in the event of a nucleophilic attack, the repulsion can be in potentially negative MEP areas. In addition, in the event of an electrophilic attack, the attraction may be to keto oxygen and the nitro group, while the greater the repulsion may be to the $-NH_2$. The negative region indicates the photostability of the compounds.

4. Conclusions

Modification of chemical structures can improve the charge transfer, optical and electronic properties. These properties were tuned by substituting the electron donor

and acceptor groups. These compounds were examined by B3LYP/6-31+G**, which allows a reliable estimate and analysis of the electronic structures of sulfur, nitrogen, and oxygen-containing organic molecules. The absorption wavelengths were estimated at the TD-B3LYP/6-31+G** level. The properties of donor– π –bridge–acceptor and acceptor– π –bridge–acceptor Schiff base compounds were explored. The substitution of -NO₂ into the furan at the 5th-position in Compound 3 leads to red shift in the absorption spectra as compared to other molecules. The smaller hole reorganization energy value of Compound 3 would have an advantage to develop its hole intrinsic mobility. The smaller electron reorganization energy value for Compound 4 as compared to other counterparts would lead to better electron charge transfer ability. The results indicated that the designed Schiff base compounds would be good for organic electronic device applications, having competence as *n*-type (Compound 3), *p*-type (Compound 4), and balanced hole as well as electron transport materials (Compounds 1/2).

Author Contributions: Conceptualization, A.I.; methodology, A.G.A.-S. and A.I.; software, A.I.; validation, A.K. and A.G.A.-S.; formal analysis, A.K.; investigation, A.G.A.-S.; resources, A.I.; data curation, A.K.; writing—original draft preparation, A.K.; writing—review and editing, A.I.; visualization, A.G.A.-S.; supervision, A.I.; project administration, A.I.; funding acquisition, A.I. All authors have read and agreed to the published version of the manuscript.

Funding: We are grateful to King Abdulaziz City for Science and Technology (KACST), Riyadh, Saudi Arabia for funding this Project under Grant number: 12-ADV2976-07-R.

Institutional Review Board Statement: Not applicable.

Informed Consent Statement: Not applicable.

Data Availability Statement: Not applicable.

Acknowledgments: We are grateful to King Abdulaziz City for Science and Technology (KACST), Riyadh, Saudi Arabia for funding this Project under Grant number: 12-ADV2976-07-R.

Conflicts of Interest: The authors declare no conflict of interest.

References

1. Reimers, J.; Picconatto, C.; Ellenbogen, J. (Eds.) *Molecular Electronics III (Annals of the New York Academy of Sciences)*; 2003. Available online: <https://www.nyas.org/annals/molecular-electronics-iii/> (accessed on 11 December 2021).
2. Tour, J. *Molecular Electronics*; World Scientific: Singapore, 2003.
3. Cunimberti, G.; Fagas, G.; Richter, K. (Eds.) *Introducing Molecular Electronics*; Lecture Notes in Physics; Springer: Berlin/Heidelberg, Germany, 2005.
4. Kaltenbrunner, M.; White, M.S.; Głowacki, E.D.; Sekitani, T.; Someya, T.; Sarıçiftçi, N.S.; Bauer, S. Ultrathin and lightweight organic solar cells with high flexibility. *Nat. Commun.* **2012**, *3*, 770. [[CrossRef](#)] [[PubMed](#)]
5. Irfan, A.; Al-Sehemi, A.G.; Al-Assiri, M.S. Push–pull effect on the electronic, optical and charge transport properties of the benzo[2,3-*b*]thiophene derivatives as efficient multifunctional materials. *Comput. Theor. Chem.* **2014**, *1031*, 76–82. [[CrossRef](#)]
6. Szlachcic, P.; Danel, K.S.; Gryl, M.; Stadnicka, K.; Usatenko, Z.; Nosidlak, N.; Lewińska, G.; Sanetra, J.; Kuźnik, W. Organic light emitting diodes (OLED) based on helical structures containing 7-membered fused rings. *Dyes Pigm.* **2015**, *114*, 184–195. [[CrossRef](#)]
7. Marks, T.J.; Hersam, M.C. Materials science: Semiconductors grown large and thin. *Nature* **2015**, *520*, 631–632. [[CrossRef](#)]
8. Beaujuge, P.M.; Fréchet, J.M.J. Molecular design and ordering effects in π -functional materials for transistor and solar cell applications. *J. Am. Chem. Soc.* **2011**, *133*, 20009–20029. [[CrossRef](#)]
9. Wang, Y.; Sun, L.; Wang, C.; Yang, F.; Ren, X.; Zhang, X.; Dong, H.; Hu, W. Organic crystalline materials in flexible electronics. *Chem. Soc. Rev.* **2019**, *48*, 1492–1530. [[CrossRef](#)] [[PubMed](#)]
10. Wang, C.; Dong, H.; Jiang, L.; Hu, W. Organic semiconductor crystals. *Chem. Soc. Rev.* **2018**, *47*, 422–500. [[CrossRef](#)]
11. Surendar, P.; Pooventhiran, T.; Rajam, S.; Rao, D.J.; Manigandan, N.; Irfan, A.; Thomas, R. Organic quasi-liquid Schiff bases from biomolecules: Synthesis, structure and quantum mechanical studies. *Biointerface Res. Appl. Chem.* **2023**, *13*, 107. [[CrossRef](#)]
12. Zhao, K.; Yu, F.; Liu, W.; Huang, Y.; Said, A.A.; Li, Y.; Zhang, Q. Unexpected synthesis, properties, and nonvolatile memory device application of imidazole-fused azaacenes. *J. Org. Chem.* **2020**, *85*, 101–107. [[CrossRef](#)]
13. Yi, W.; Zhao, S.; Sun, H.; Kan, Y.; Shi, J.; Wan, S.; Li, C.; Wang, H. Isomers of organic semiconductors based on dithienothiophenes: The effect of sulphur atoms positions on the intermolecular interactions and field-effect performances. *J. Mater. Chem. C* **2015**, *3*, 10856–10861. [[CrossRef](#)]

14. Pajak, A.K.; Kotowicz, S.; Gnida, P.; Małecki, J.G.; Ciemiega, A.; Tuczak, A.; Jung, J.; Schab-Balcerzak, E. Synthesis and characterization of new conjugated azomethines end-capped with amino-thiophene-3,4-dicarboxylic acid diethyl ester. *Int. J. Mol. Sci.* **2022**, *23*, 8160. [CrossRef]
15. Grigoras, M.; Catanescu, C.O. Imine oligomers and polymer. *J. Macromol. Sci. Part C* **2004**, *44*, 131–173. [CrossRef]
16. Isik, D.; Santato, C.; Barik, S.; Skene, W.G. Charge-carrier transport in thin films of π -conjugated thiopheno-azomethines. *Org. Electron.* **2012**, *13*, 3022–3031. [CrossRef]
17. Sicard, L.; Navarathne, D.; Skalski, T.; Skene, W.G. On-substrate preparation of an electroactive conjugated polyazomethine from solution-processable monomers and its application in electrochromic devices. *Adv. Funct. Mater.* **2013**, *23*, 3549–3559. [CrossRef]
18. Jeevadason, A.W.; Murugavel, K.K.; Neelakantan, M.A. Review on Schiff bases and their metal complexes as organic photovoltaic materials. *Renew. Sustain. Energy Rev.* **2014**, *36*, 220–227. [CrossRef]
19. García-López, M.C.; Muñoz-Flores, B.M.; Jiménez-Pérez, V.M.; Moggio, I.; Arias, E.; Chan-Navarro, R.; Santillan, R. Santillan, Synthesis and photophysical characterization of organotin compounds derived from Schiff bases for organic light emitting diodes. *Dyes Pigment.* **2014**, *106*, 188–196. [CrossRef]
20. Ivanova, B.B.; Spiteller, M. Optical and nonlinear optical properties of new Schiff's bases: Experimental versus theoretical study of inclusion interactions. *J. Incl. Phenom. Macrocycl. Chem.* **2013**, *75*, 211–221. [CrossRef]
21. Sidir, Y.G.; Arslan, C.; Berber, H.; Sidir, I. The electronic structure, solvatochromism, and electric dipole moments of new schiff base derivatives using absorbance and fluorescence spectra. *Struc. Chem.* **2019**, *30*, 835–851. [CrossRef]
22. Zhang, L.; Zhang, Q.; Ren, H.; Yan, H.; Zhang, J.; Zhang, H.; Gu, J. Calculation of band gap in long alkyl-substituted heterocyclic-thiophene-conjugated polymers with electron donor–acceptor fragment. *Sol. Energy Mater. Sol. Cells* **2008**, *92*, 581–587. [CrossRef]
23. Hassanali, A.A.; Li, T.; Zhong, D.; Singer, S.J. A molecular dynamics study of lys-trp-lys: Structure and dynamics in solution following photoexcitation. *J. Phy. Chem. B* **2006**, *110*, 10497–10508. [CrossRef] [PubMed]
24. Irfan, A.; Imran, M.; Thomas, R.; Basra, M.A.R.; Ullah, S.; Al-Sehemi, A.G.; Assiri, M.A. Exploring the effect of oligothiophene and acene cores on the optoelectronic properties and enhancing *p*- and *n*-type ability of semiconductor materials. *J. Sulfur Chem.* **2021**, *42*, 180–192. [CrossRef]
25. Irfan, A. Push-pull effect on the charge transport characteristics in v-shaped organic semiconductor materials. *Bull. Mater. Sci.* **2021**, *44*, 43. [CrossRef]
26. Wazzan, N.; Irfan, A. Promising architectures modifying the d- π -a architecture of 2,3-dipentylidithieno[3,2-f:2',3'-h]quinoxaline-based dye as efficient sensitizers in dye-sensitized solar cells: A DFT study. *Mater. Sci. Semiconduc. Process.* **2020**, *120*, 105260. [CrossRef]
27. Kumar, M.U.; Jeyakumari, A.P.; Suresh, M. Senthilkumar Chandran, G Vinitha. *Mater. Res. Express* **2019**, *6*, 075102.
28. Ermis, E. Synthesis, spectroscopic characterization and DFT calculations of novel Schiff base containing thiophene ring. *J. Mol. Struct.* **2018**, *1156*, 91–104. [CrossRef]
29. Kohn, W.; Becke, A.D.; Parr, R.G. Density functional theory of electronic structure. *J. Phys. Chem.* **1996**, *100*, 12974–12980. [CrossRef]
30. Becke, A.D. Density-functional thermochemistry. Iii. The role of exact exchange. *J. Chem. Phys.* **1993**, *98*, 5648–5652. [CrossRef]
31. Miehlich, B.; Savin, A.; Stoll, H.; Preuss, H. Results obtained with the correlation energy density functionals of becke and lee, yang and parr. *Chem. Phys. Lett.* **1989**, *157*, 200–206. [CrossRef]
32. Tang, S.-S.; Liu, J.-B.; Chen, G.; Jin, R.-F. Theoretical study on electronic and charge transfer properties of oligo[8]thiophene and its circular, hooped, and helical derivatives. *Chin. J. Struct. Chem.* **2014**, *33*, 104–114.
33. Li, P.; Bu, Y.; Ai, H. Theoretical determinations of ionization potential and electron affinity of glycineamide using density functional theory. *J. Phys. Chem. A* **2004**, *108*, 1200–1207. [CrossRef]
34. Furche, F.; Ahlrichs, R. Adiabatic time-dependent density functional methods for excited state properties. *J. Chem. Phys.* **2002**, *117*, 7433–7447. [CrossRef]
35. Frisch, M.J.; Schlegel, H.B.; Scuseria, G.E.; Robb, M.A.; Cheeseman, J.R.; Scalmani, G.; Barone, V.; Mennucci, B.; Petersson, G.A.; Nakatsuji, H.; et al. *Gaussian 09, Revision A.01*; Gaussian Inc.: Wallingford, CT, USA, 2016.
36. Takano, Y.; Houk, K.N. Benchmarking the conductor-like polarizable continuum model (cpcm) for aqueous solvation free energies of neutral and ionic organic molecules. *J. Chem. Theo. Comp.* **2005**, *1*, 70–77. [CrossRef]
37. Some data from Handbook of Chemistry and Physics. Available online: http://www2.chemistry.msu.edu/faculty/harrison/cem483/work_functions.pdf (accessed on 10 January 2022).
38. Sonar, P.; Singh, S.P.; Leclère, P.; Surin, M.; Lazzaroni, R.; Lin, T.T.; Dodabalapur, A.; Sellinger, A. Synthesis, characterization and comparative study of thiophene–benzothiadiazole based donor–acceptor–donor (D-A-D) materials. *J. Mater. Chem.* **2009**, *19*, 3228–3237. [CrossRef]
39. Nikolka, M.; Nasrallah, I.; Rose, B.; Ravva, M.K.; Broch, K.; Sadhanala, A.; Harkin, D.; Charmet, J.; Hurhangee, M.; Brown, A.; et al. High operational and environmental stability of high-mobility conjugated polymer field-effect transistors through the use of molecular additives. *Nature Mater.* **2017**, *16*, 356–362. [CrossRef]
40. de Leeuw, D.M.; Simenon, M.M.J.; Brown, A.R.; Einerhand, R.E.F. Stability of *n*-type doped conducting polymers and consequences for polymeric microelectronic devices. *Synth. Met.* **1997**, *87*, 53–59. [CrossRef]
41. Abbaszadeh, D.; Kunz, A.; Kotadiya, N.B.; Mondal, A.; Andrienko, D.; Michels, J.J.; Wetzelaer, G.-J.A.H.; Blom, P.W.M. Electron trapping in conjugated polymers. *Chem. Mater.* **2019**, *31*, 6380–6386. [CrossRef]

42. Usta, H.; Risko, C.; Wang, Z.; Huang, H.; Deliomeroglu, M.K.; Zhukhovitskiy, A.; Facchetti, A.; Marks, T.J. Design, synthesis, and characterization of ladder-type molecules and polymers. Air-stable, solution-processable *n*-channel and ambipolar semiconductors for thin-film transistors via experiment and theory. *J. Am. Chem. Soc.* **2009**, *131*, 5586–5608. [[CrossRef](#)] [[PubMed](#)]
43. Felscia, U.R.; Rajkumar, B.J.M.; Mary, M.B. Charge transport properties of pyrene and its derivatives: Optoelectronic and nonlinear optical applications. *J. Mater. Sci.* **2018**, *53*, 15213–15225. [[CrossRef](#)]
44. Yang, G.; Su, Z.; Qin, C. Theoretical study on the second-order nonlinear optical properties of asymmetric spiro-silabifluorene derivatives. *J. Phy. Chem. A* **2006**, *110*, 4817–4821. [[CrossRef](#)]
45. Wazzan, N.; El-Shishtawy, R.M.; Irfan, A. DFT and TD-DFT calculations of the electronic structures and photophysical properties of newly designed pyrene-core arylamine derivatives as hole-transporting materials for perovskite solar cells. *Theor. Chem. Acc.* **2017**, *137*, 9. [[CrossRef](#)]
46. Wazzan, N.; Irfan, A. Theoretical study of triphenylamine-based organic dyes with mono-, di-, and tri-anchoring groups for dye-sensitized solar cells. *Org. Electron.* **2018**, *63*, 328–342. [[CrossRef](#)]
47. Brédas, J.-L.; Beljonne, D.; Coropceanu, V.; Cornil, J. Charge-transfer and energy-transfer processes in π -conjugated oligomers and polymers: A molecular picture. *Chem. Rev.* **2004**, *104*, 4971–5004. [[CrossRef](#)] [[PubMed](#)]
48. Chai, W.; Jin, R. Theoretical investigations into optical and charge transfer properties of donor-acceptor 1,8-naphthalimide derivatives as possible organic light-emitting materials. *J. Mol. Struct.* **2016**, *1103*, 177–182. [[CrossRef](#)]
49. Gruhn, N.E.; da Silva Filho, D.A.; Bill, T.G.; Malagoli, M.; Coropceanu, V.; Kahn, A.; Brédas, J.-L. The vibrational reorganization energy in pentacene: Molecular influences on charge transport. *J. Am. Chem. Soc.* **2002**, *124*, 7918–7919. [[CrossRef](#)]